Electrochemical Vapor Deposition of a Graded Titanium Oxide-Yttria Stabilized Zirconia Layer

by

Andrew Gouldstone

Submitted to the Department of Materials Science and Engineering
in partial fulfillment of the requirements for the degree of

Bachelor of Science in Materials Science and Engineering

at the

MASSACHUSETTS INSTITUTE OF TECHNOLOGY

June 1996

Author.....
Department of Materials Science and Engineering
May 10, 1996

Certified by.....
Uday B. Pal
Associate Professor of Chemical Processing of Materials
Thesis Supervisor

Certified by.....
Subra Suresh
Professor of Metallurgy
Thesis Supervisor

Accepted by.....
David K. Roylance
Associate Professor of Materials Engineering
Department of Materials Science and Engineering

Electrochemical Vapor Deposition of a Graded Titanium Oxide/Yttria Stabilized Zirconia (YSZ) Layer

by

Andrew Gouldstone

Submitted to the Department of Materials Science and Engineering on May 10, 1996, in partial fulfillment of the requirements for the degree of Bachelor of Science in Materials Science and Engineering.

Abstract

Functionally graded materials (FGM's) are layered structures of graded composition to avoid sharp interfaces between constituent layers. Electrochemical Vapor Deposition (EVD) is explored as a process for fabricating a titanium oxide (TiO_2) - yttria stabilized zirconia (YSZ) FGM. Thermodynamic favorability of processes involved and viability of products are analyzed. Porous substrates are fabricated and characterized using direct and indirect methods. Oxide precursors are mixed in accordance with results of thermodynamic evaluation. Experimental set-up of the EVD reactor is reviewed and system flaws discussed. Successful fabrication of these materials could lead to their eventual use in solid oxide fuel cells.

Thesis Supervisor: Uday B. Pal
Title: Associate Professor of Metallurgy, DMSE

Thesis Supervisor: Subra Suresh
Title: Professor of Metallurgy, DMSE

Acknowledgements

The author wishes to thank the following individuals without whom the production of this work would have been considerably more difficult.

Mr. Won Sang Bae

Professor Kyung-Muk Cho

Dr. Kuo-Chih Chou

Mr. George LaBonte

Mr. Peter Ragone

Mr. Sridhar Seetharaman

I would also like to thank my two advisors, Professor Uday Pal and Professor Subra Suresh, for providing me with this project and the motivation to complete it.

Table of Contents

Table of Figures

Table of Tables

Chapter 1

Introduction

1.1 Solid Oxide Fuel Cells

Solid oxide fuel cells (SOFC's) are an alternative energy source to the current combustion mechanisms of the 20th century. Power outputs of 30kW have been achieved with small modular cell arrays. SOFC's are "clean," in that they produce non-polluting by-products by converting chemical energy directly into electrical energy. With new recycling systems, by-products of SOFC fuels can be used elsewhere. However, before SOFC's can be put to widespread use, they must decrease their relatively high cost per watt. This decrease can be accomplished by making SOFC's more efficient through materials design, and also by cutting processing costs.

SOFC's are constructed of materials of different conductivity types. Ionic conductivity (σ_i) is the ability of a material to conduct ions, usually via diffusion. Electronic conductivity (σ_e) is the ability to conduct electrons. If $\sigma_i >> \sigma_e$, the material is an ionic conductor. If $\sigma_i << \sigma_e$, the material is an electronic conductor. If σ_i is comparable to σ_e, the material is a mixed conductor. One common design of the SOFC is the flat plate design, in which the ionically conducting electrolyte is sandwiched between a cathode and an anode, both electronically conductive (Fig. 1).

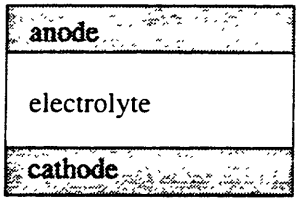

Fig 1. Flat plate design of an SOFC

The anode is exposed to a hydrogen atmosphere and the cathode to an oxygen atmosphere. The different pressures of oxygen on either side of the cell set up a chemical potential. The oxygen is ionized at the cathode-oxygen-electrolyte interface, with the addition of 4 electrons for every O_2 molecule, by the following equation:

$$O_2 + 4e^- \text{----> } 2O^{2-}$$

The ions are transported through the solid electrolyte via vacancy diffusion, until they reach the hydrogen-anode-electrolyte interface, at which point they combine with hydrogen to make water vapor, by the following equation:

$$2O_2\text{-} + 2H_2\text{---> } 2H_2O + 4e^-$$

A schematic of this process is displayed in Fig.2.[1] The fuel cell in a circuit attached to a load produces a current. The power produced is the product of this current and the open circuit voltage, determined by the difference in oxygen partial pressure across the electrolyte. This process has the potential to be more efficient. The gas-electron-electrolyte reactions take place only at small "triple points" where all three meet (Fig. 3a). The gas comes from one source, the electrons come

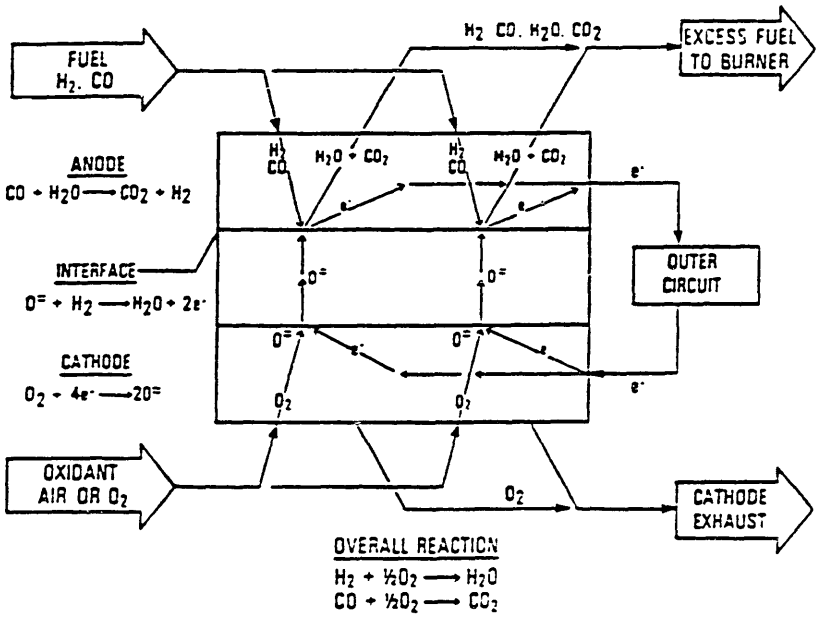

Fig 2. Schematic of SOFC Operation

from the electronically conductive electrode, and the ions travel through the electrolyte. Materials that combine electronic and ionic conductivity at the surface of the electrolyte would increase its efficiency. Yttria stabilized zirconia (YSZ), an ionic conductor, is the current material of choice for the electrolyte in SOFC's. When doped with Titanium oxide (TiO_2), an electronic conductor, the YSZ becomes mixed conducting.[2] This mixed conductivity would allow a greater reaction area at the surface of the cell electrolyte (Fig. 3b). However, two important operating constraints of the fuel cell must be considered in order to select processing techniques for this electrolyte design.

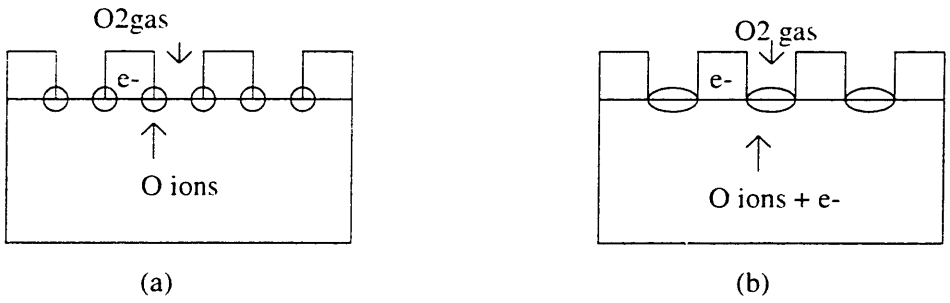

Figure 3. a)An ionically conducting electrolyte, with the reaction taking place at points. b)A mixed conducting electrolyte, with the reaction occurring over a greater area.

The first condition is that the solid electrolyte must be able to conduct ions. A mixed conductor, while increasing efficiency at the gas surface, would decrease overall ionic conductivity. Where the electrons and gas are no longer in contact with the electrolyte, mixed conduction is neither necessary or favorable. Therefore, the TiO_2 doping must be confined to a thin layer, on the order

of 50 microns.

The second condition is that SOFC's must be operated at a temperature of 800°C, in order for the electrolyte to conduct oxygen ions. Layered structures, such as those in a SOFC are often subjected to large temperature changes, either during processing or operation. If the layers are comprised of materials with different coefficients of thermal expansion (cte), the mismatch that results upon changing the temperature can lead to high thermal stresses at the interface between the two materials (Fig 4a). These stresses can lead to cracking and failure of the system.[3]

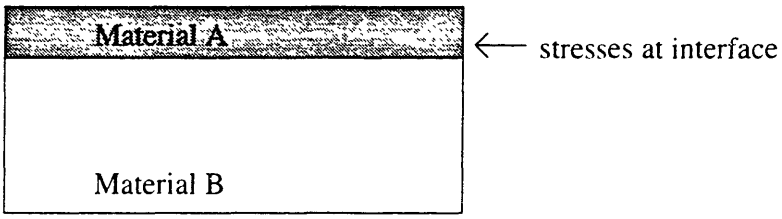

Fig 4a. Layered structure containing thermal stresses at the interface due to mismatch.

1.2 Functionally Graded Materials

Functionally graded materials (FGM) are a proposed solution to the problem of thermal stresses, and also provide a means of varying conductivity with depth. Their design contains no discrete interface, but instead a varying concentration of material with distance.[4] A schematic is shown in

Fig 4b. This graded design minimizes the thermal stresses that result from two materials with dif-

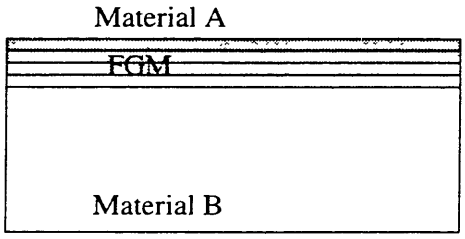

Fig 4b. FGM structure leading to decreased thermal stresses..

ferent cte's. A YSZ system in which the TiO_2 concentration varies with depth will result in lower thermal stresses than a YSZ system with a discrete layer of TiO_2 (see Results). An FGM is also favorable for the electrical properties of the SOFC system. Since electronic conductivity depends on the presence of TiO_2, this design will also "grade" conductivity, allowing a greater reaction surface area while maintaining the high ionic conductivity of the electrolyte at greater depths.. The creation of this material system is possible through electrochemical vapor deposition (EVD.) This research project will explore the possibility of using the EVD process to fabricate such a functionally graded material system.

Chapter 2

Background

2.1 EVD Process

EVD is a deposition process in which gaseous halides react with oxygen to form oxides on a

porous substrate at high temperature. Halides are flown on one side of the substrate, and oxygen is flown on the other. The first stage is the chemical vapor deposition (CVD) stage, in which the oxygen and halides meet in the pores of the substrate, producing oxides and filling the pores, making the substrate fully dense (Fig 5a).

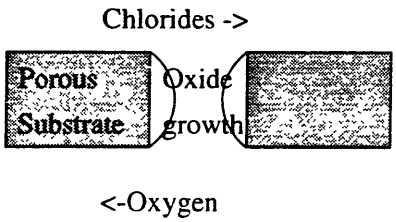

Fig 5a. CVD stage with oxide growth within the susbtrate pores.

When these pores are filled, the second stage, so called the EVD stage begins, in which the oxygen partial pressure difference across the substrate drives oxygen ion diffusion through the substrate, allowing it to continue reacting with halides. Oxygen is diffused as ions of O^{2-} and electrons are transported in the opposite direction to balance charge.[4] This reaction forms a dense oxide layer on the surface of the substrate (Fig 5b).

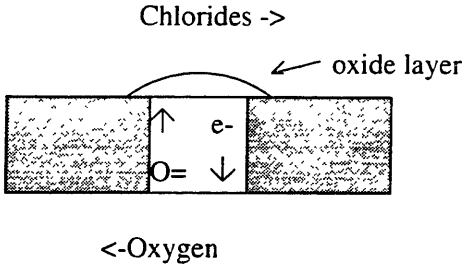

Fig 5b. EVD stage with diffusion of oxygen ions across deposited oxide and reaction with chlorides to produce dense oxide layer.

Research by Pal et al showed that deposition of an oxide via EVD is limited by transport of the

minority carriers through the oxide. For an ionic oxide

$$\kappa = \left((RT) / \left(2|Zo|F^2 \right) \right) \int_{PiiO_2}^{PiO_2} \sigma_e d\ln PO_2$$

and for an electronic oxide

$$\kappa = \left((RT) / \left(2|Zo|F^2 \right) \right) \int_{PiiO_2}^{PiO_2} (\sigma_1 + \sigma_3) d\ln PO_2$$

where κ is the parabolic growth rate constant, σ_e is the electronic conductivity, σ_1 is the conductivity of the cations, σ_3 is the conductivity of the anions, F is Faraday's constant, Zo is the valence of the oxygen anions, R is the gas constant and T is the temperature in degrees Kelvin.[5]

Halides necessary for deposition can be created by two proven methods. The first involves flowing argon over chlorides at 150°C to produce vapor phase chlorides. The second method, which was chosen for this experiment, creates chlorides by flowing chlorine over oxide precursors at 1200°C. Rationale for this choice is included in the Discussion section.

Chapter 3

Theoretical Analysis

3.1 Thermodynamic Analysis

A layer of TiO_2-doped YSZ is deposited by flowing oxygen on one side of the substrate and

$ZrCl_4$, YCl_3 and $TiCl_4$ on the other side. Vapor phase halides were to be created by flowing chlorine over YSZ and TiO_2 at high temperatures. HSC Chemistry software was used to determine the optimum method for producing these chlorides at the deposition temperature of 1200°C.

The following reactant combinations were examined to determine the equilibrium amount of vapor phase chlorides present at an overall reactor pressure of 0.01 torr.

-A_aO_b + $bCl_2(g)$, varying temperature from 500°C to 2100°C

-A_aO_b + $bCl_2(g)$ at 1200°C, varying moles of $Cl_2(g)$ from 0.2 to 8.2

-A_aO_b + bC + $bCl_2(g)$, varying temperature from 500°C to 2100°C

-A_aO_b + bC + $bCl_2(g)$ at 1200°C, varying moles of $Cl_2(g)$ from 0.2 to 8.2

(where a and b are subscripts for cation A and oxygen, respectively)

Plots of equilibrium concentrations for oxides ZrO_2, Y_2O_3 and TiO_2 are displayed in Appendix A.

At 1200°C, the optimum amounts of halides are produced by the following ratios of reactants through the overall reactions

$ZrO_2 + 2Cl_2(g) + 2C \rightarrow ZrCl_4(g) + 2CO(g)$

$Y_2O_3 + 3Cl_2(g) + 3C \rightarrow 2YCl_3(g) + 3CO(g)$

$TiO_2 + 2Cl_2(g) + 2C \rightarrow TiCl_4(g) + 2CO(g)$

3.2 Stress Analysis Using Multitherm Software

The stresses existing in a YSZ-(15%TiO_2-85%YSZ) bilayered material with a discrete interface were compared to those of a YSZ-FGM-(15%TiO_2-85%YSZ) system.(Fig 6) Stresses were com-

pared for systems after cooling from the deposition temperature of 1200°C to room temperature, and after one cycle of "fuel cell" operation at 800°C.(Fig 7)

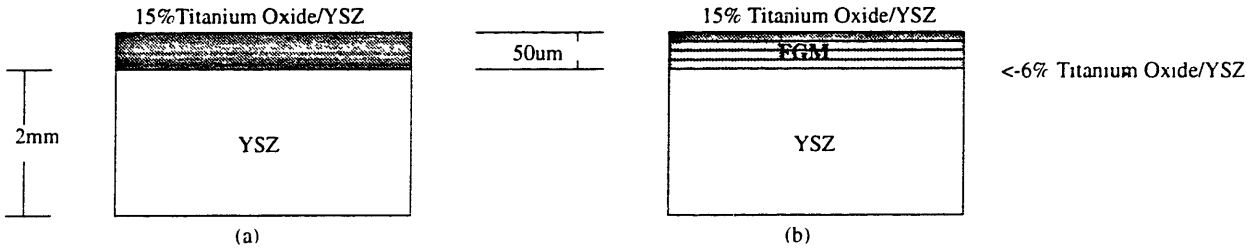

Fig 6. Schematic of the layered matierals used for Multitherm analysis.
a)Discrete layer of Titanium Oxide on YSZ. b)FGM.

Fig. 7 Thermal Cycling of Bilayer and FGM

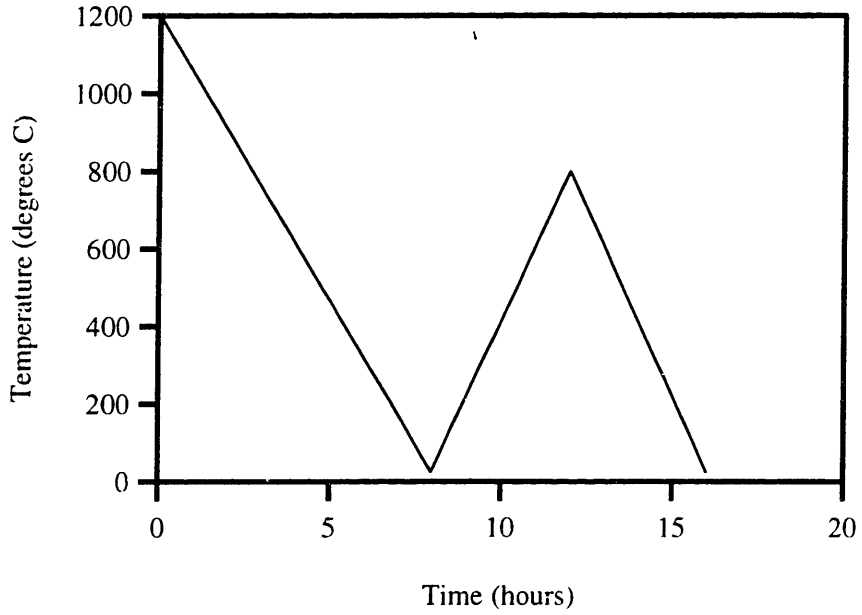

Both oxides were treated as linear elastic materials and so the only applicable thermomechanical properties were Young's Modulus E, coefficient of thermal expansion α,(at $O^{o}C$), $d\alpha/dT$ and Poisson's ratio ν, which was taken to be 0.3. Properties of the compounds were determined by using a volume weighted average of the two materials. Properties of the selected materials for the bilayered system are displayed in Table 1. Those for the FGM are displayed in Table 2.

Table 1: Materials in Bilayered System for Multitherm Analysis

Material	Thickness	E(GPa)	$\alpha(x10^{-6}/K)$	$d\alpha/dT$
YSZ	2mm	206	10	0
15%TiO_2/85%YSZ	50um	217.55	9.775	0

Table 2: Materials in FGM for Multitherm Analysis

Material	Thickness	E(GPa)	$\alpha(x10^{-6}/K)$	$d\alpha/dT$
YSZ	2mm	206	10	0
FGM	50um	varies lin-early	varies lin-early	0

2.3 TiO_2-ZrO_2 phase diagram

The TiO_2-ZrO_2 phase diagram is displayed in Fig 8. This diagram shows that for a 15%/85% TiO_2/YSZ mixture, an intermediate phase, $ZrTiO_4$ is formed. In order to take advantage of the different conductivities of the deposited oxides, TiO_2 and YSZ must exist as two distinct phases.

TiO_2–ZrO_2

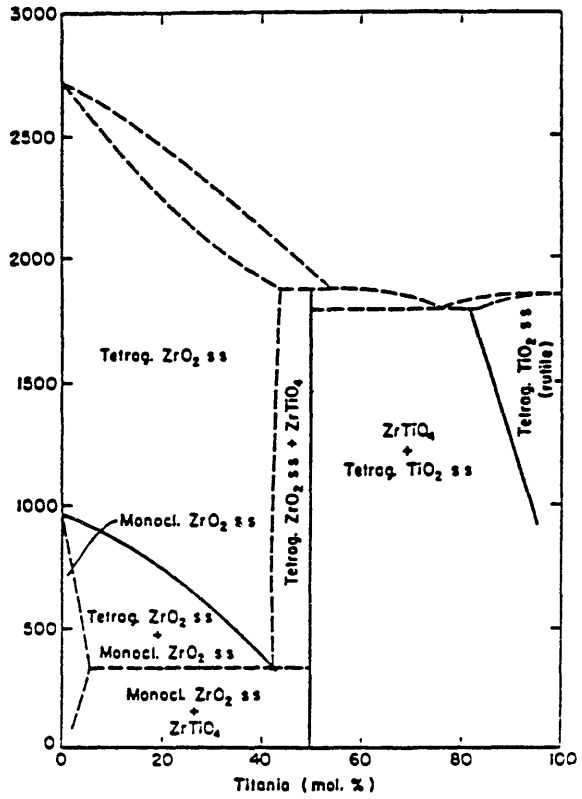

FIG. 369.—System TiO_2–ZrO_2; proposed.

Frank H. Brown, Jr., and Pol Duwez, *J. Am. Ceram. Soc.*, 37 [3] 132 (1954).

Fig. 8 The TiO_2/ZrO_2 Phase Diagram

This compound is neither a good ionic or electronic conductor, and must be avoided for a successful FGM.

Chapter 4

Experimental Procedure

The procedure for fabrication of FGM via EVD involves the fabrication of porous YSZ substrates, preparation of the EVD reactor and also the PRE-EVD runs. Preparation of the reactor includes a temperature profile and a weight loss test.

4.1 Substrate Processing and Characterization

Substrates for EVD required the following characteristics: a)a thickness of 1-2.5mm, b)20% open porosity and c)homogeneous porosity with no cracks. YSZ powder was mixed with polyvinyl alcohol (PVA) as a binder,cellulose acetate as a pore former and polyethylene glycol and stearic acid as lubricants. The powder was pressed in a 1" die at 2500 psi for 8 minutes, removed, dried in an oven at 70^{o}C for 3 hours and sintered at 1400^{o}C in air for four hours. The sintering profile is displayed in Fig 9. Bulk density of substrates was determined by measuring the volume of the sintered discs (with calipers), weighing them and comparing calculated densities with the theoretical density of fully dense YSZ. Homogeneity of porosity was characterized by a direct method, cross-sectional analysis in an optical microscope. Finally, mercury porosimetry, an indirect method, was performed on substrates to provide a quantitative description of pore size distribution, and also to distinguish closed pores from open pores. Two porosimetry runs were performed on each sample. A low pressure run evacuated a penetrometer containing the sample, and immersed the sample in mercury, to confirm its bulk density. A high pressure run applied increas-

ing oil pressures up to 50000psi. in order to force mercury into smaller pores and determine pore size distribution.

Fig.9. Sintering Schedule of YSZ Substrates

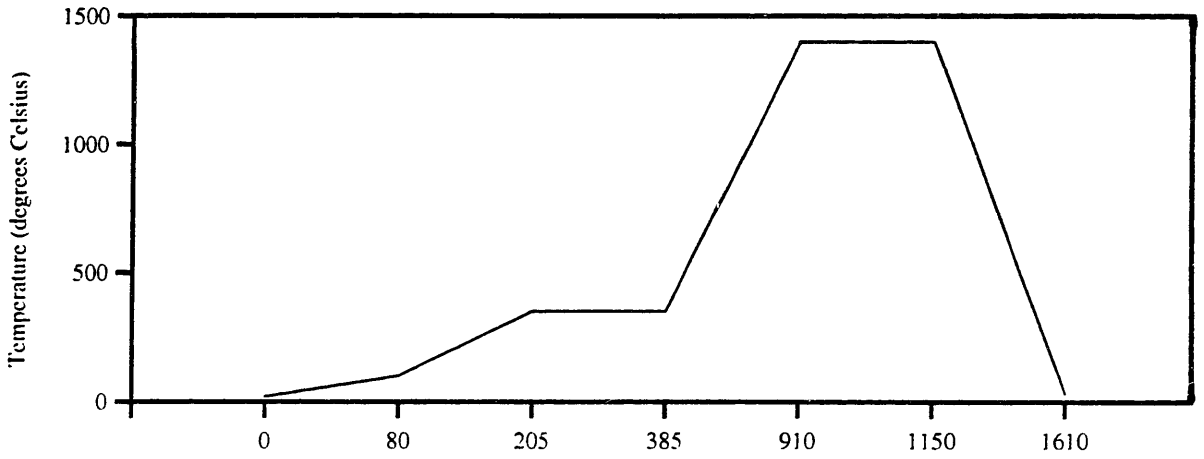

4.2 Setup of Reactor

4.2.1 Halide Supply

Halides were provided by flowing chlorine gas over oxide precursors at 1200°C. The precursors were prepared by mixing YSZ powder with carbon black in a 3:1 molar ratio and TiO_2 powder with carbon black in a 3:1 molar ratio. (Compositions were chosen based on results of HSC analysis) Powders were ball milled for 24 hours, mixed with deionized water and pressed under light pressure for 1 minute to provide a mechanically stable green body. Green body weights were around 40g. The oxide/carbon mixtures were then sintered in a reducing atmosphere of forming gas (95%N_2/5%H_2) for four hours, removed, and then crushed into chunks.

Precursor chunks were placed in a 25" graphite cartridge assembly which contained the oxides in

the hot zone of the reactor. (Fig 10)

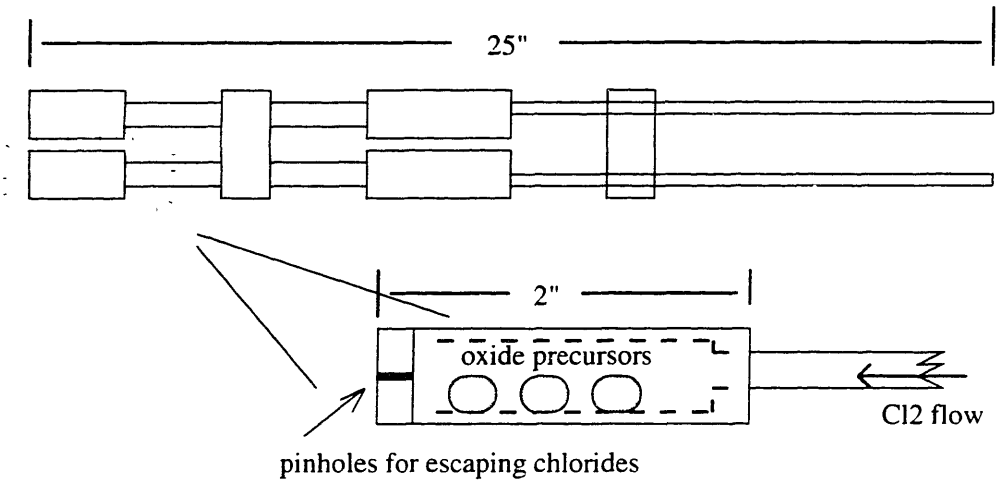

Fig10. Graphite Cartridge Assembly for Oxide Precursor Chunks

Chlorine gas was supplied to the oxides through the assembly. Argon (a carrier gas) and hydrogen (to react with Cl_2 after deposition) were flown outside the assembly. Graphite baffles were placed ahead of the assembly to promote complete mixing of the resulting $ZrCl_4$, YCl_3 and $TiCl_4$.

4.2.2 Oxygen Supply

The porous substrate was sealed in a 3/4" zirconia tube with a PVA/YSZ sealant. The tube extended 22" into the reactor, placing the substrate in the hot zone. An oxygen inlet and outlet were placed inside this tube.(Fig.11)

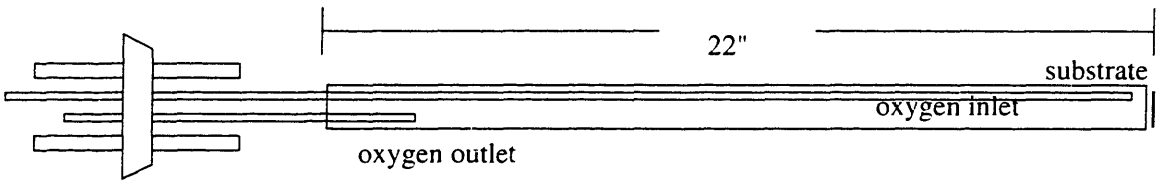

The oxygen outlet and a tube leading into the reactor through a valve were connected to one side of a manometer partially filled with mercury (Fig.12). The other side of the manometer was connected directly to the reactor. The purpose of the manometer was to determine the completeness of the CVD stage of the deposition process. As pores are filled in the substrate, pressure builds up in the holder tube. When the valve leading to the reactor is closed, the manometer displays a pressure difference between the inside and the outside of the tube. The rate at which the mercury levels change provide a qualitative description of how much of the porosity has been filled.

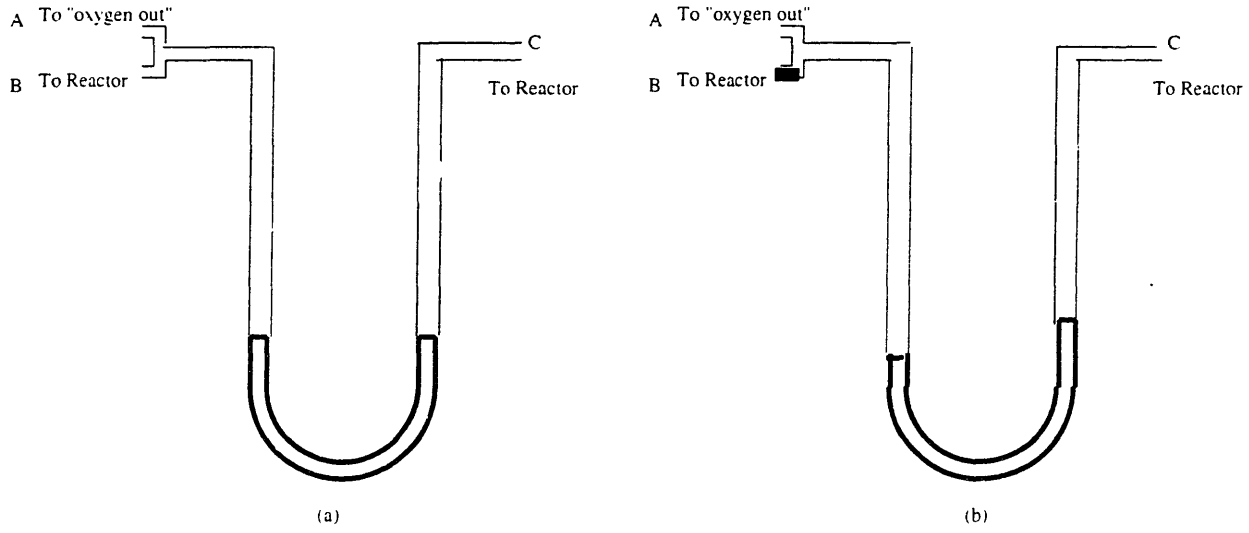

Fig 12 The Manometer is used to determine the completeness of the CVD stage of the EVD process a) When A, B and C are open, the pressure on either side of the manometer is the vacuum pressure and the mercury levels are equal b)When A and C are open and B is closed, the pressure building up in the substrate holder tube causes the mercury levels to shift The rate of shift upon closing gives an indication of when the CVD stage is complete

4.2.3 Temperature Profile

The temperature profile determines the section of the furnace along which the temperature does

not vary with position, designated the "hot zone." This was taken by ramping the reactor furnace up to 1200°C and using a thermocouple to measure the temperature at 1" increments. A graph of the results for a 60" furnace tube are displayed in Fig.13. This figure shows that the hot zone extends from 22" to 40" into the reactor. This "hot zone" is where both the formation of chlorides and deposition of oxides must be carried out.

Fig. 13. EVD Furnace Temperature Profile

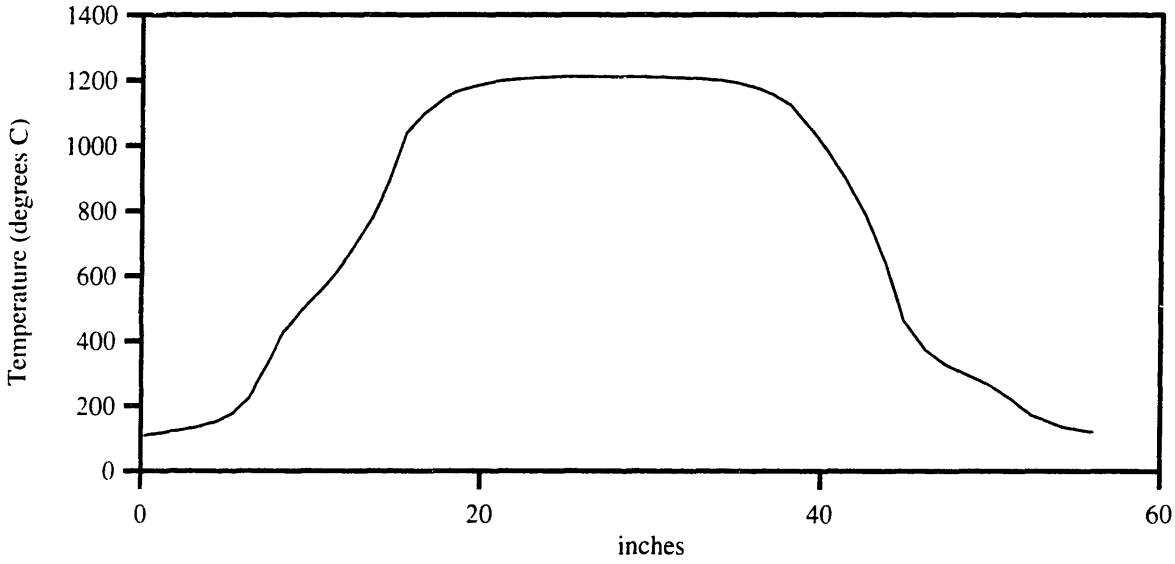

4.3 Weight loss test

A weight loss test was performed in order to determine the kinetic factors of the following reactions of the oxides to chlorides at 1200°C.

a) $ZrO_2 + 2Cl_2(g) + 2C \rightarrow ZrCl_4(g) + 2CO(g)$

b) $Y2O_3 + 3Cl_2(g) + 3C \rightarrow 2YCl_3(g) + 3CO(g)$

c) $TiO_2 + 2Cl_2(g) + 2C \rightarrow TiCl_4(g) + 2CO(g)$

At 1200°C if oxides reacted with chlorine gas, the mass of the oxides would decrease. Chlorine was flown over the YSZ at a flow rate of 20cc/min and over the TiO_2 at 12cc/min. The masses of the oxides before and after the run were compared, and from the weight loss and the presence of chlorides in the reactor after the experiment, it was concluded that chlorides were being produced at 1200°C. (The presence of chlorides was determined by sight and smell.) The total time of the weight loss test was 30 minutes. From the weight loss and the chlorides present within this time, it was concluded that reactions (a), (b), and (c) were thermodynamically and kinetically favorable at 1200°C.

4.4 PRE-EVD Runs

An EVD run was a full day operation. In the morning, the reactor tube was lined with grafoil and the graphite cylinders, and attached to the pyrex cold trap, which led to the vacuum pump. After all outside connections were confirmed as leaktight (i.e, the reactor can pull a vacuum of 0.2 torr), the substrate holder was placed into the reactor, and its oxygen inlet and outlet, along with tubes leading to the reactor, were attached. This was again checked for leaks. Finally, the flowmeters for the chlorine, argon and hydrogen were attached and checked for leaks. Once the system was leak-tight, oxide precursors were weighed out (about 3 to 4g) and placed into the cartridges, which were put into the reactor behind the baffles. The vacuum was started and the reactor was ramped up by the following schedule to the deposition temperature of 1200°C. (Fig.14)

Fig.14 Ramp Schedule for EVD Run

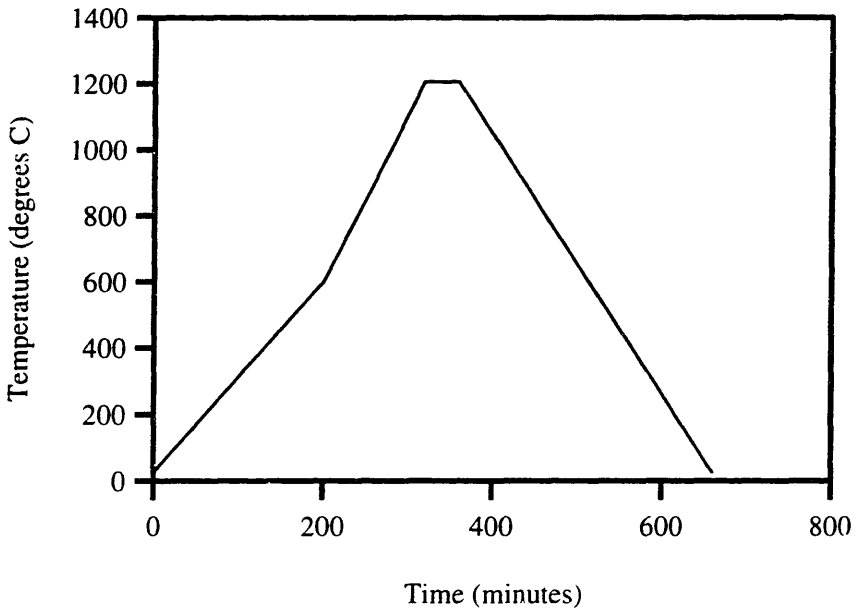

At 600°C, argon flow was started at 150cc/min and hydrogen flow was started at 30cc/min. At 1000°C, the cold trap was immersed in liquid nitrogen. Once the reactor reached 1200°C, chlorine flow to the YSZ began at 30cc/min and oxygen flow to the substrate began at 30cc/min. The manometer was periodically checked every 2 minutes to monitor the porosity of the substrate. After 15 minutes, chlorine flow to the TiO_2 began at 5-10cc/min and all flows continued for another 25 minutes. After 40 minutes total, porosity was checked with the manometer and oxygen and chlorine gas flows were halted. Ramp down of the reactor was initiated and the vacuum was left on overnight to pull any halides into the cold trap.

The following morning, the reactor had reached room temperature and the vacuum was shut down. The substrate was removed and examined for any deposition. The oxide precursors were removed, weighed and checked for evidence of chloride formation. All parts of the reactor were then removed to a fume hood, and flushed with water for 3 hours. The alumina furnace tube was

rinsed with acetone. Findings from the runs are found in the Discussion section.

Chapter 5

Results

5.1 Multitherm

Stress plots of the different materials systems are displayed in Fig. 15a)after cooling down from the deposition temperature of 1200°C, b)after heating to 800°C and c)after cooling down to room temperature. After cooling to room temperature after deposition, stresses of 75 MPa exist at the discrete interface, leading to possible separation. Maximum stresses in the FGM exist at the surface of the doped layer, away from the interface. Maximum stresses are decreased after heating to 800°C, and then return to 75 MPa at the interface in the discretely layered material and 75 MPa at the surface for the FGM (with virtually no stress at the interface).

5.2 Characterization of Substrates

Results of the mercury porosimetry runs are displayed in Appendix B. After the low pressure run, the density of the substrates was found to be approximately 85%. From the high pressure run, the median pore size was determined to be approximately 1 micron. Data from initial mass/volume measurements of the substrates and optical microscope photos (Fig. 16) of the substrates pointed to densities around 75% with average pore size of 10 microns.

Fig 15a. Stress plots after cooling from 1200°C for i)bilayered system and ii)FGM

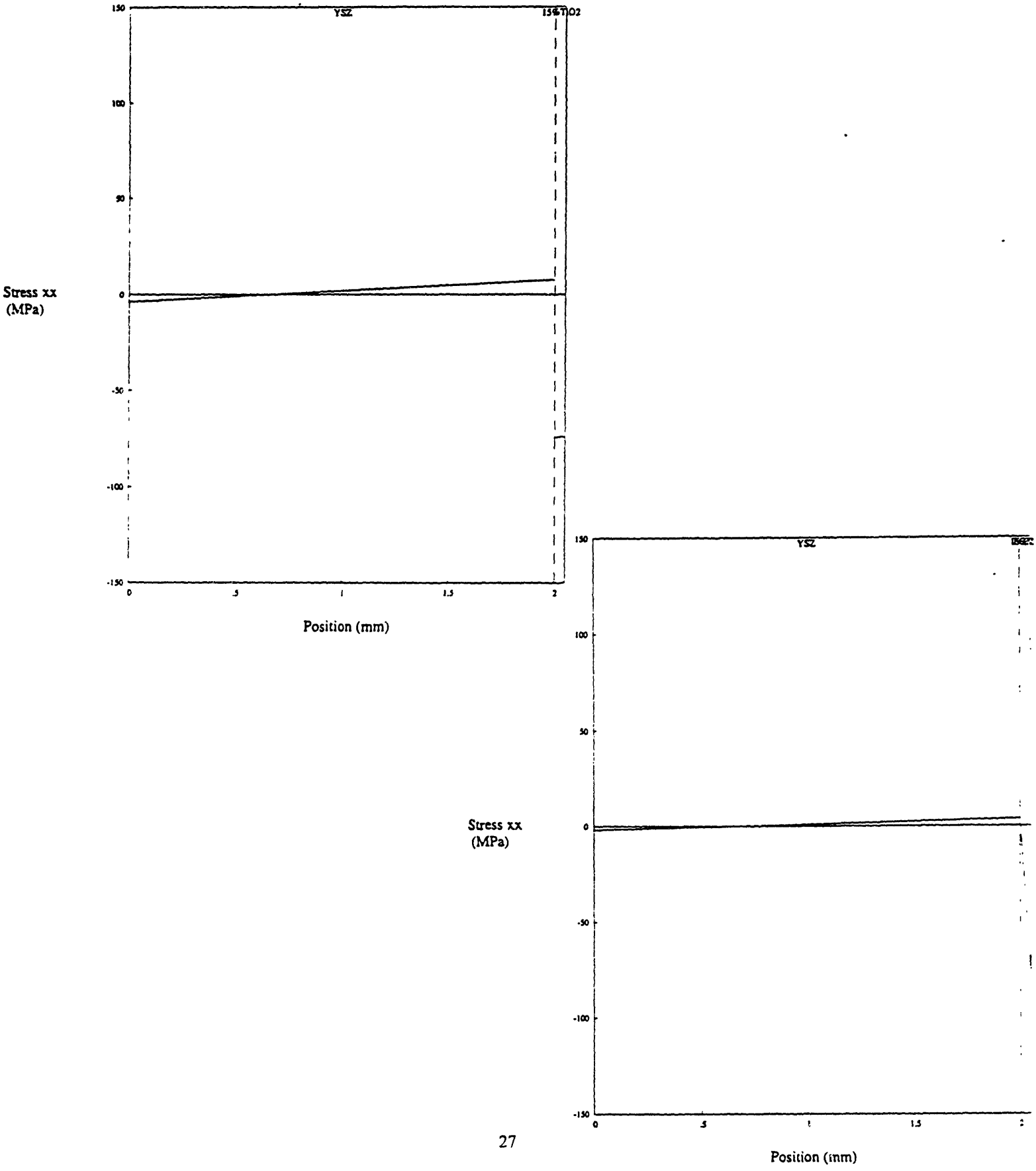

Fig 15b. Stress plots after heating to 800°C for i)bilayered system and ii)FGM

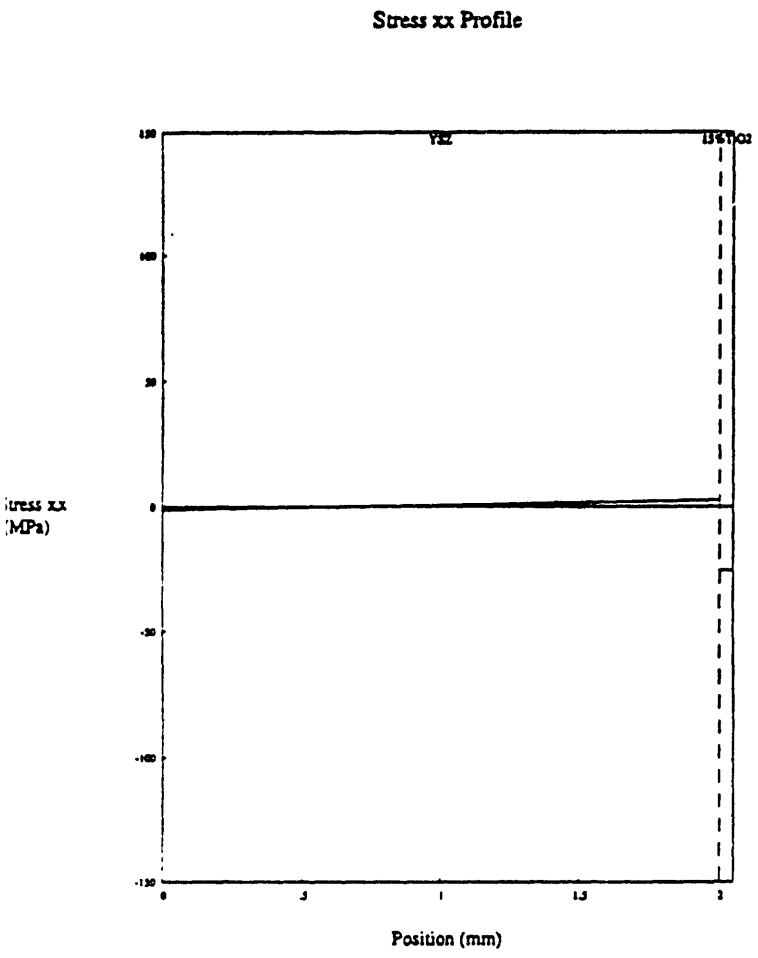

i)bilayered system

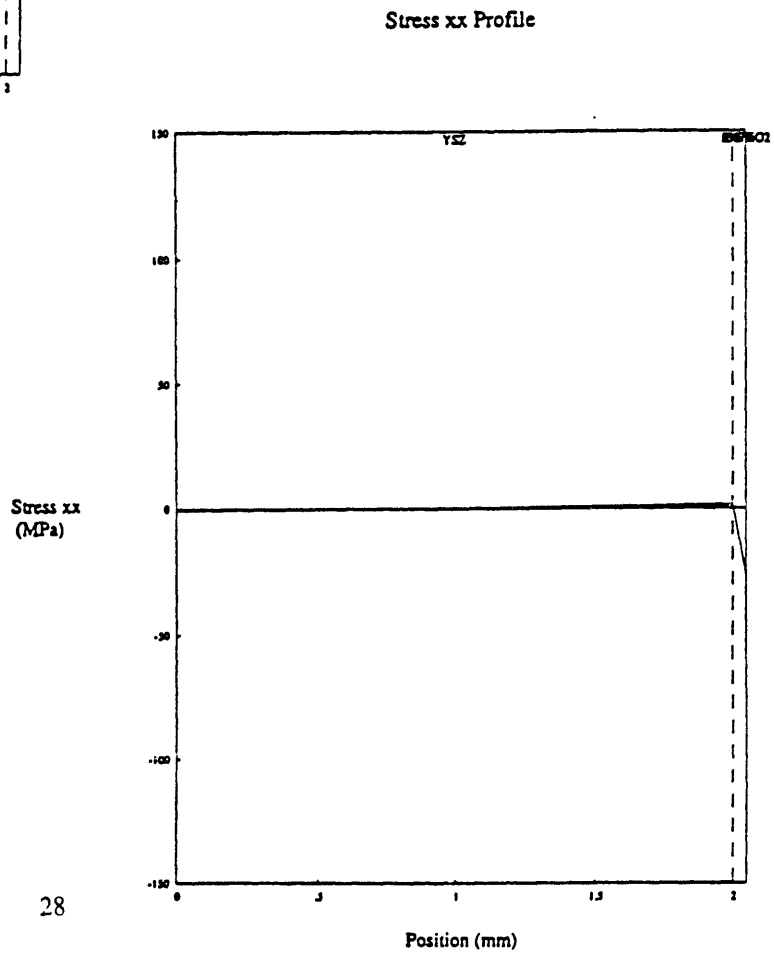

ii)FGM

Fig 15c. Stress plots after cooling from 800°C for i)bilayered system and ii)FGM

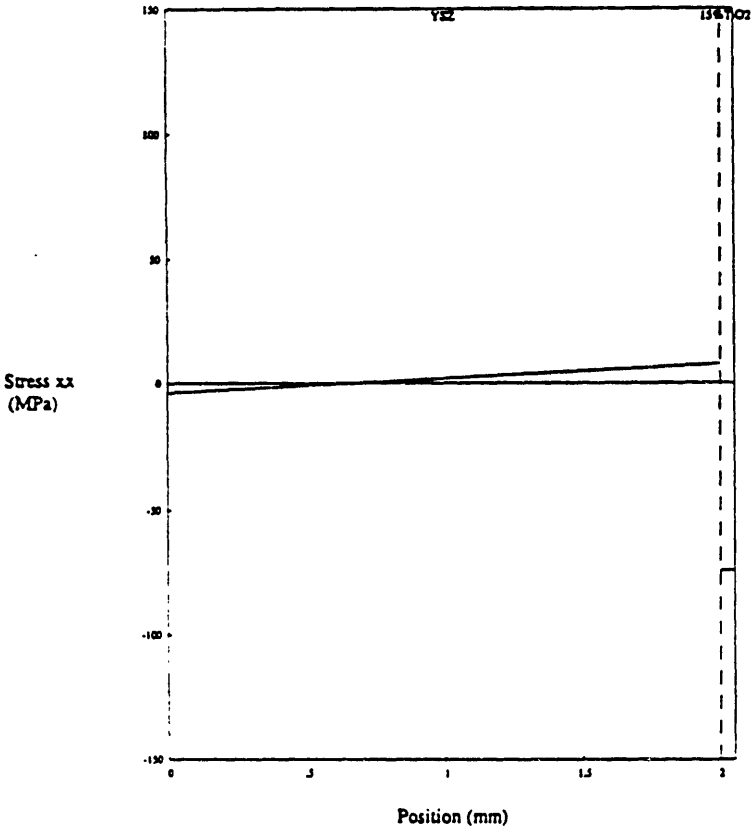

i)bilayered system

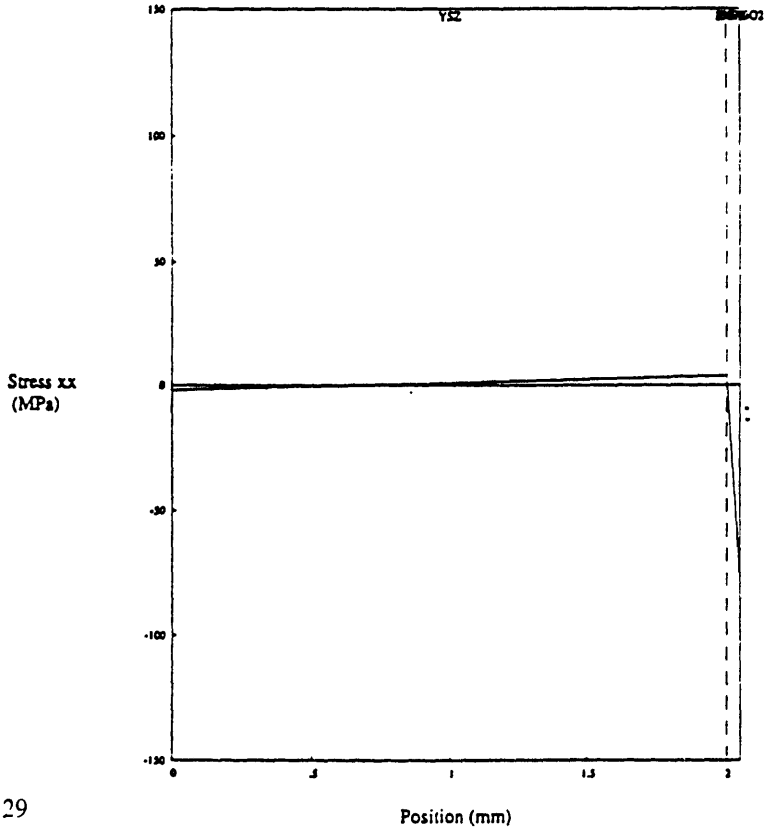

ii)FGM

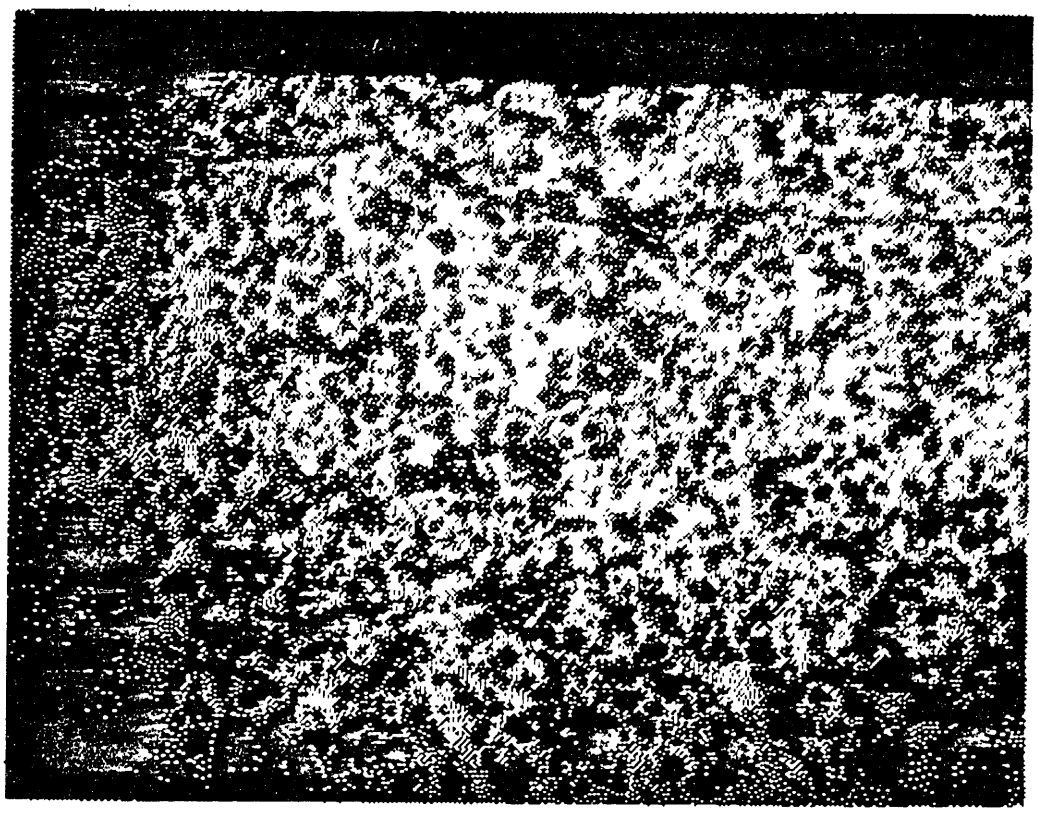

Fig 16. Cross section of YSZ substrate in an optical microscope (100x)

Chapter 6

Discussion

6.1 Substrates

Compilation of data from direct and indirect methods of substrate characterization indicated that a percentage of the porosity was closed porosity. Pores were also smaller than expected. Substrates met the required characteristics for deposition, and porosimetry was a new technique suggested late in the experiment, so new substrates could not be designed. However, the apparent homoge-

neity of the porosity indicated by both characterization methods shows that mixing and preparation of powders was sufficient. Percentage of closed porosity could be decreased simply by increasing the volume ratio of cellulose to YSZ powder in the initial composition. More pores would have a higher probability of remaining connected. Pore sizes could be made larger by firing at a lower temperature, around 1300°C, to promote more coarsening and less densifying of the substrates. Any lower firing temperature could lead to sintering during EVD runs and is not recommended.

6.2 Chloride Source

Two methods for producing chlorides were mentioned. The process of flowing argon over chlorides at 150°C has been used for successful deposition.[5] It involves no chlorine gas and no corrosives outside the reactor during operation. However, for a process to produce an FGM, precise control of chloride production is necessary. This method does not allow such control, as vapor pressure of chlorides under vacuum is difficult to calculate, and (referring to Fig. 8) a precise temperature away from the hot zone is very difficult to control in the EVD reactor, which further decreases control over chloride vapor pressure. The method of flowing chlorine over oxides has been successfully tested, but not for production of an FGM.[10] However, the flow of chlorides would be much more easily regulated in this second process, hence its selection for this experiment, in which flow must be altered regularly.

6.3 PRE-EVD Runs

After each run, the substrate was examined for any deposition. The reactor was examined for evidence of $ZrCl_4$, YCl_3 and $TiCl_4$. Weight loss of powder was performed. After the initial weight

loss test discussed in the procedure section, no weight loss of YSZ nor TiO_2 was detected. Throughout all the runs, this was the underlying problem. Chlorides were not being produced so no deposition could possibly be taking place. Throughout the entire experiment, various possibilities for the failure of the oxides to react with chlorine were entertained. Since weight loss had been achieved in the first run and temperature and oxide/carbon composition had not been altered, thermodynamic and kinetic reasons were eventually ruled out and system failure was explored. The chlorine delivery system into the reactor was not leaking, as the vacuum necessary for deposition was maintained inside the reactor, and no chlorine smell was detected in the laboratory or the fume hood containing the flowmeters. A possible leak in the graphite delivery system was investigated, perhaps due to oxidation of the cartridge stems, causing them to become porous. Following this theory, a new assembly was constructed, and confirmed (after testing with air) to be sufficiently leakproof. However, this provided no solution to the problem. It was confirmed that chlorine was indeed flowing into the reactor by the presence of a small amount (~10ml) of liquid at the bottom of the cold trap after the EVD run. This liquid was determined to be HCl, which has a boiling point of 100°C, and exists as a liquid at the low temperature in the cold trap. Regardless, the chlorine gas was not reaching the oxides, and the problem could not be rectified in time to complete a successful deposition run.

Despite system problems which arose and could not be dealt with in the time allotted for this experiment, motivation for and theoretical success of this process still remains high. A graded material would greatly decrease dehesion problems that could upon cooling of a multilayered material. Optimum oxide precursor specifications have been realized and substrate fabrication is a reproducible process.

Chapter 7

Conclusion

A process for the fabrication of a YSZ-TiO_2 doped YSZ FGM via electrochemical vapor deposition was designed. Chlorides necessary for deposition were to be produced by flowing chlorine over oxide precursors at 1200°C. Theoretical analysis of the process and the resulting material was carried out. The optimum precursor compositions were determined, and stress analysis results for the proposed FGM were compared to results for a bilayered material. Porous YSZ substrates were manufactured and the EVD reactor was designed and set up for the deposition process. Experimental runs exposed a system flaw preventing the chlorine gas from reaching the oxide precursors. With this problem solved, deposition should be possible, along with experimental analysis of the transport properties of a graded TiO_2/YSZ film. The next step for this project is to experimentally confirm the theoretical analyses presented via successful deposition and characterization of the resulting FGM.

An experimentally viable process for deposition of a graded film could be used in the fabrication of solid oxide fuel cells. Using a cathode material as a substrate, electrolyte and anode materials could be adhered in a single processing step, greatly diminishing overall cell costs.

References

1 Minh, N. "Ceramic Fuel Cells." Journal of the American Ceramic Society, Vol 76, No. 3. 562-582 (March 1993)

2 Worrell, Wayne L. et al. "A Novel Single-Component Oxide Fuel Cell." Proceedings from the EPRI/GRI Fuel Cell Workshop on Fuel Cell Technology Research and Development, April 2-3, 1996, Tempe, Arizona.

3 Suresh, S. et al. "Elastoplastic Analysis of Thermal Cycling: Layered Materials with Sharp Interfaces." J. Mech. Phys. Solids, Vol. 42, No.6, 979-1018, 1994.

4 Suresh, S. et al. "Elastoplastic Analysis of Thermal Cycling: Layered Materials with Compositional Gradients." Acta metall. mater. Vol. 43, No. 4, 1335-1354, 1995.

5 Pal, U.B. et al. "Analysis of the Solid State Transport Involved in the Electrochemical Vapor Deposition of Binary and Ternary Oxides." High Temperature Science, Vol 32, 23-34, 1991.

6 Phase Diagrams for Ceramists, Vol VI. 1975.

7 CRC Materials Science and Engineering Handbook. Edited by James F. Shackelford. 1992 by CRC Press, London.

8 Thermophysical Properties of High Temperature Solid Materials Vol 4. Edited by Y.S. Tou-

loukian. Thermophysical Properties Research Center, Purdue University.

9 Thermophysical Properties of High Temperature Solid Materials Vol 5. Edited by Y.S. Touloukian. Thermophysical Properties Research Center, Purdue University.

10 Procedure for Fabrication of a Solid Electrolysis Cell. Westinghouse Corp. 1993

APPENDIX A. Equilibrium Plots from HSC Software

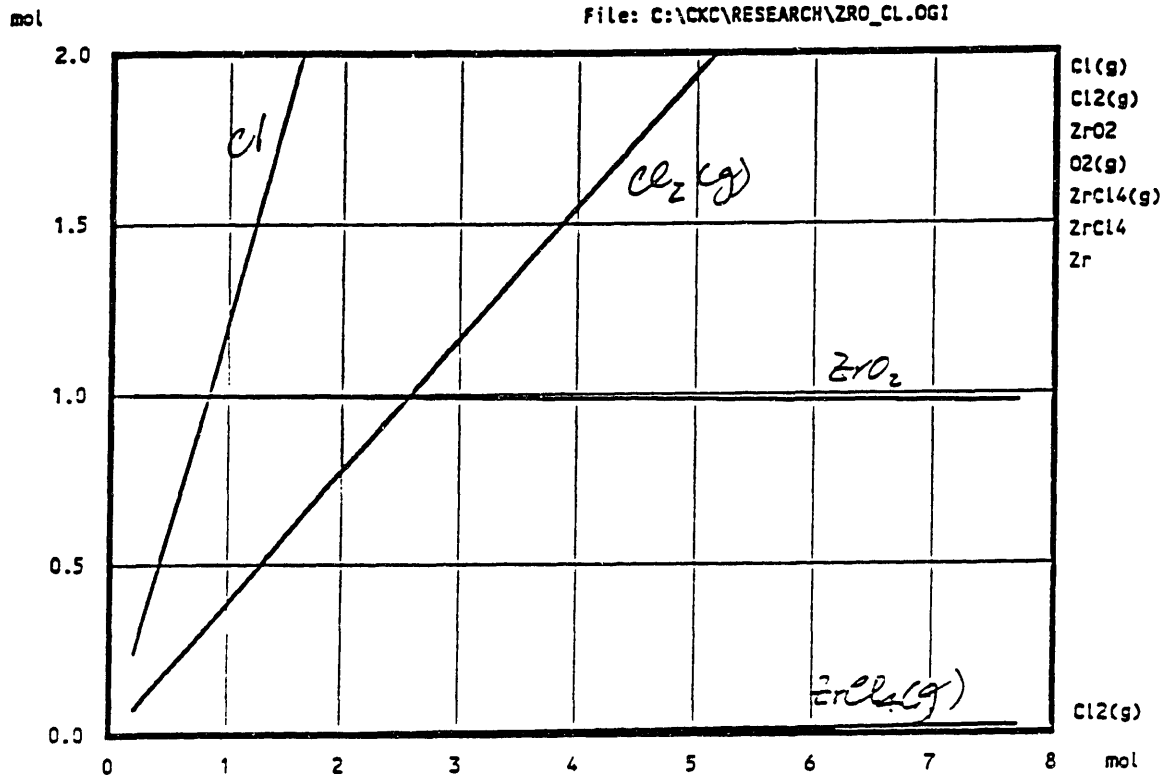

Temperature:	1473.150 K
Pressure:	0.001 bar
Raw Materials:	mol
Cl2(g)	2.0000E-01
ZrO2	1.0000E-00

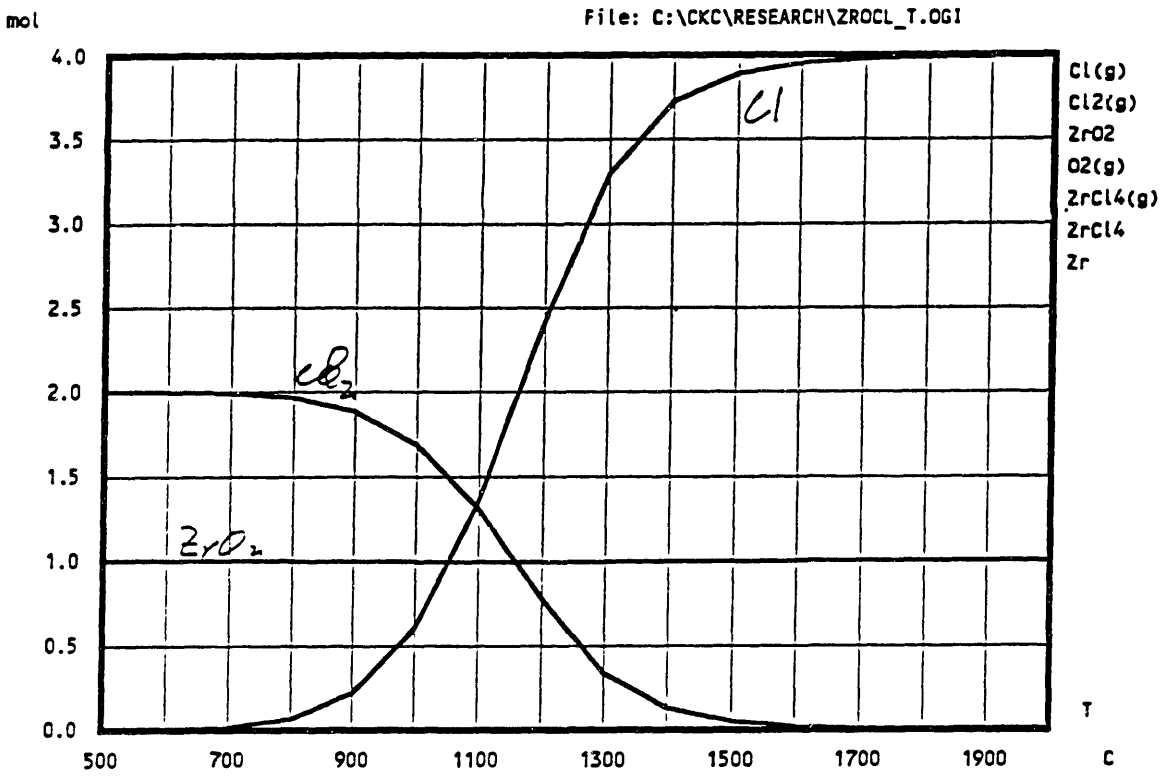

Temperature:	773.150 K
Pressure:	0.001 bar
Raw Materials:	mol
Cl2(g)	2.0000E+00
ZrO2	1.0000E+00

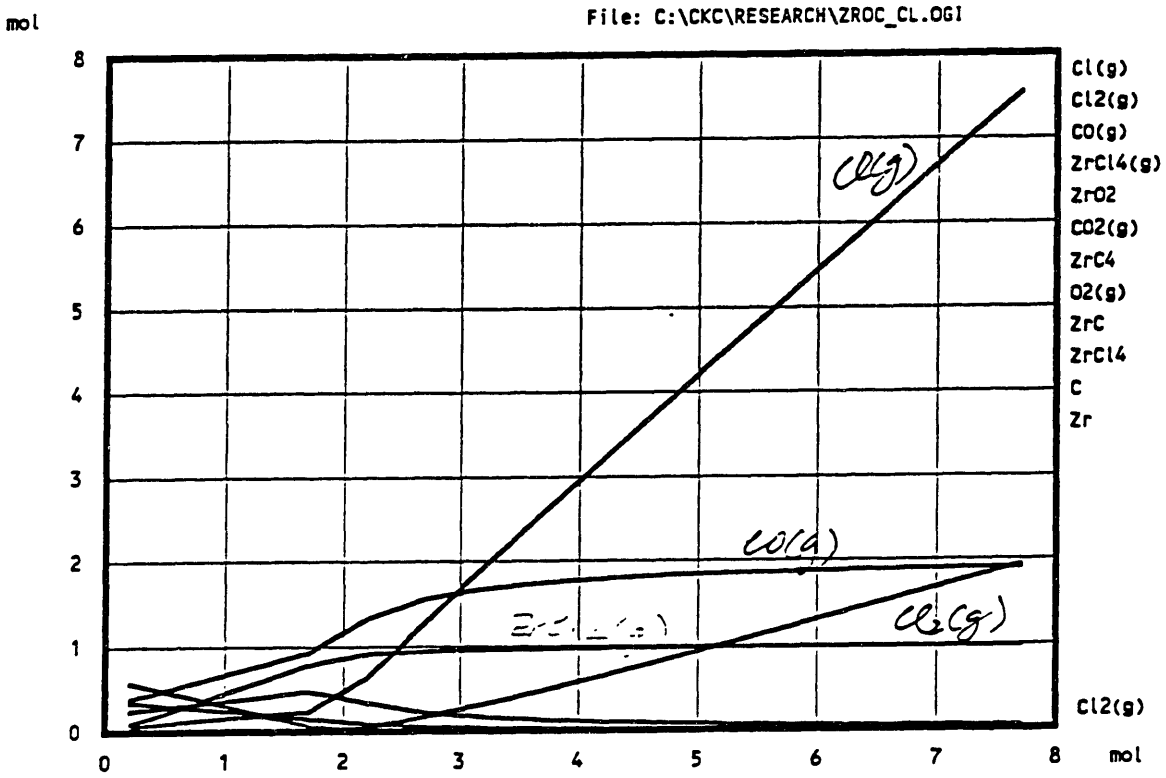

Temperature:	1473.150 K
Pressure:	0.001 bar
Raw Materials:	mol
Cl2(g)	2.0000E-01
ZrC2	1.0000E+00
C	2.0000E+00

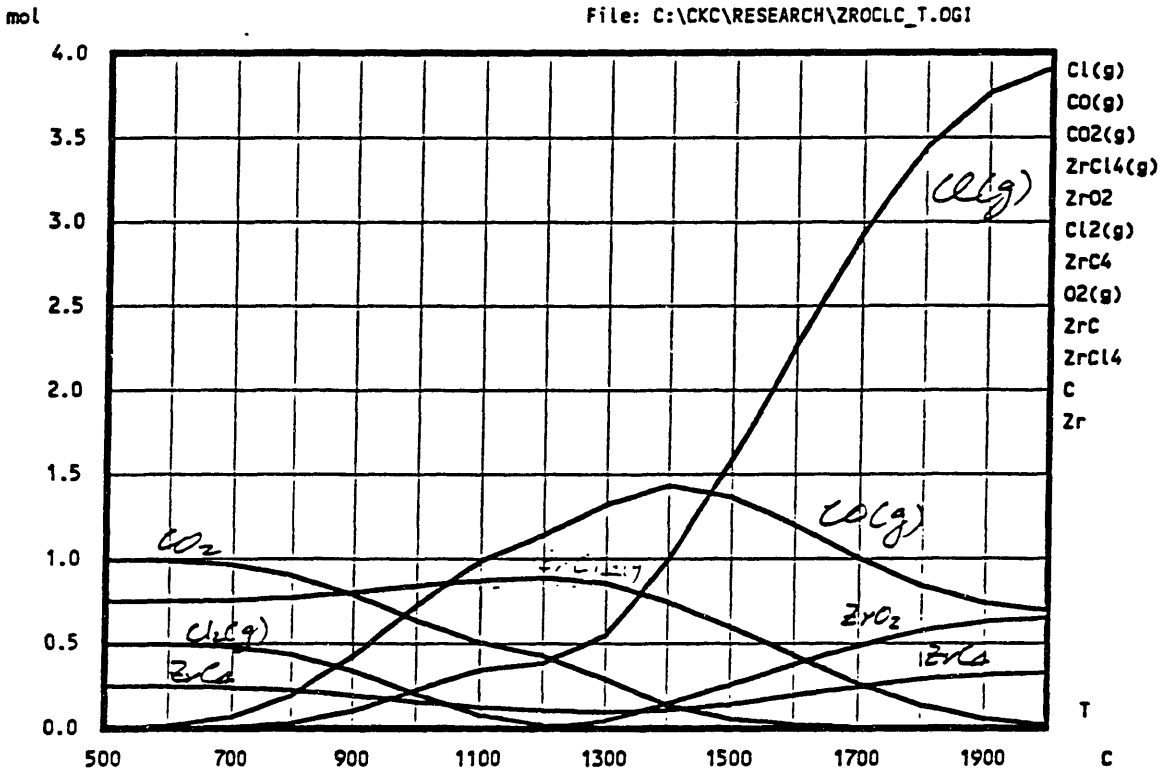

Temperature:	773.150 K
Pressure:	0.001 bar
Raw Materials:	mol
Cl2(g)	2.0000E+00
ZrO2	1.0000E+00
C	2.0000E+00

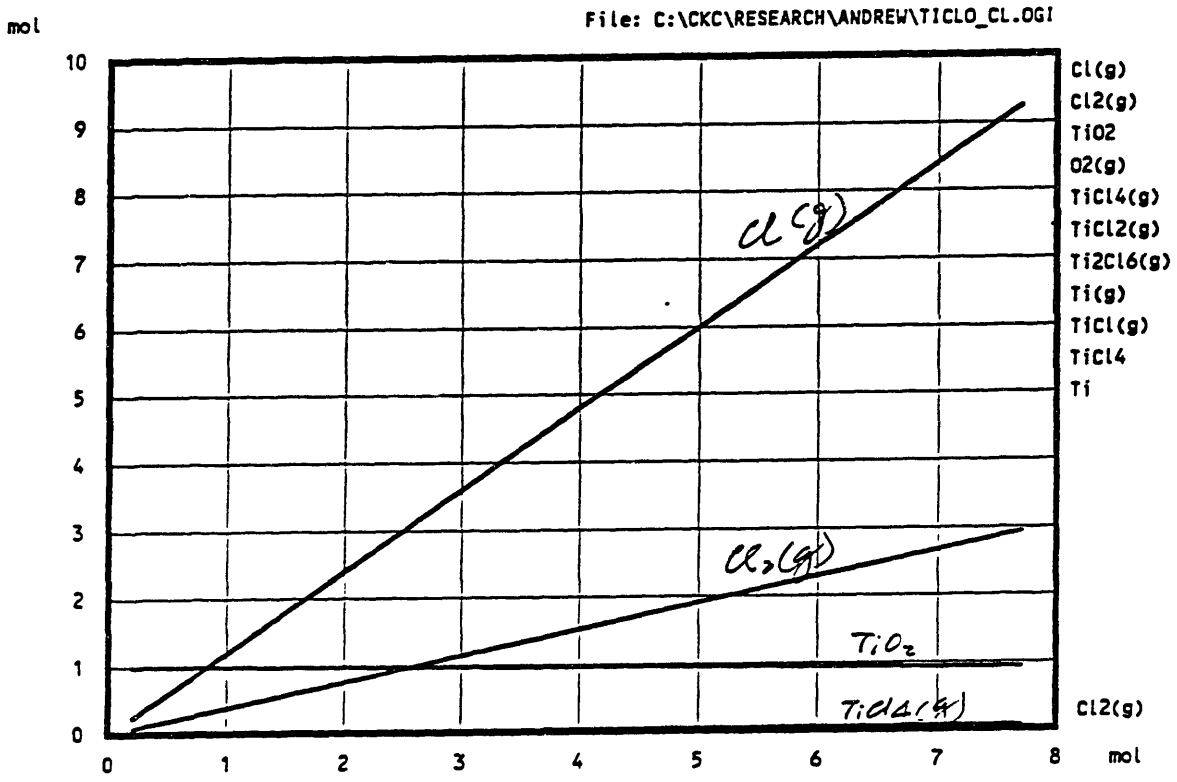

Temperature:	1473.150 K
Pressure:	0.001 bar
Raw Materials:	mol
Cl2(g)	2.0000E-01
TiO2	1.0000E+00

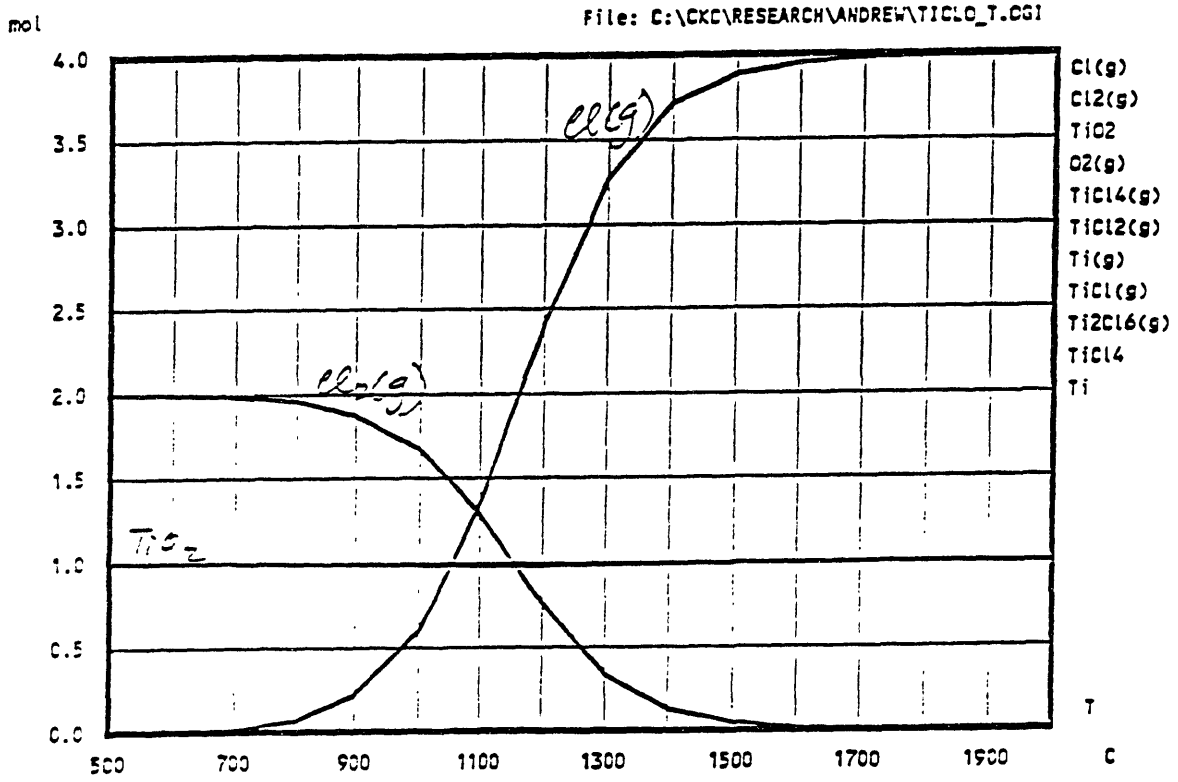

Temperature:	773.150 K
Pressure:	0.001 bar
Raw Materials:	mol
Cl2(g)	2.0000E-00
TiO2	1.0000E-00

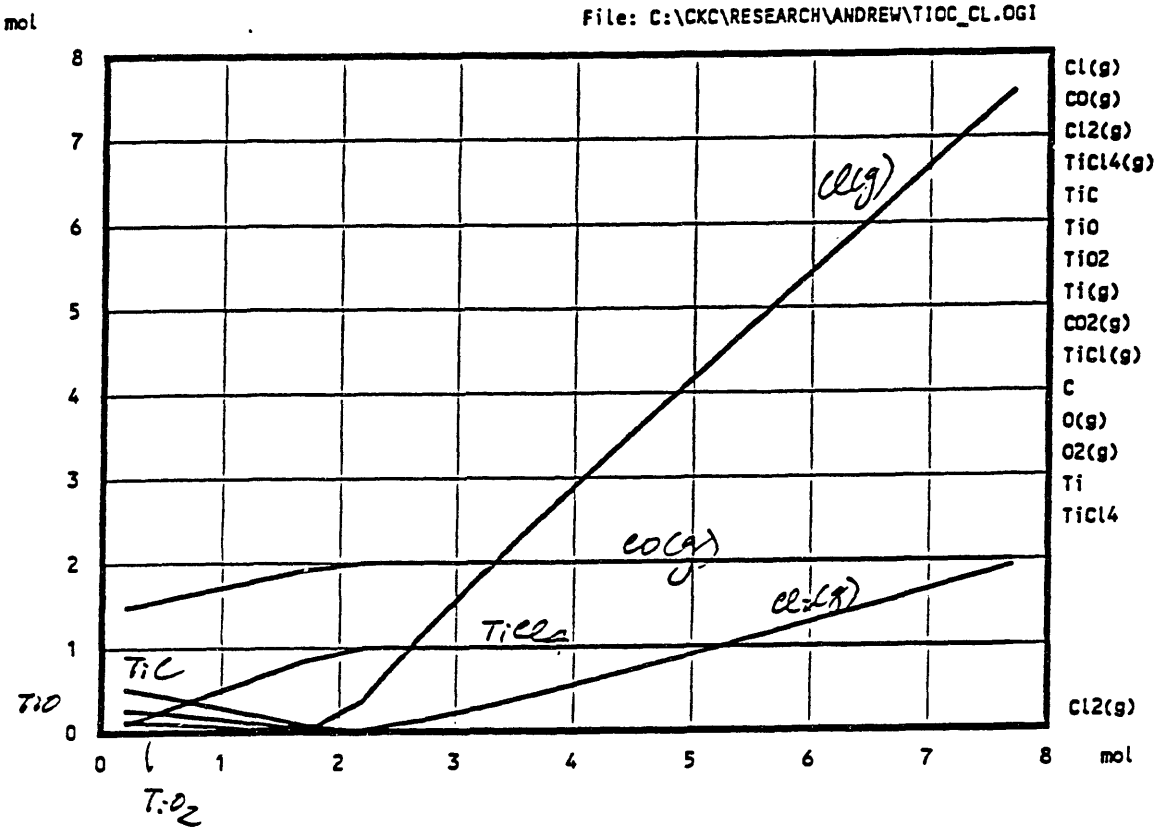

Temperature:	1473.150 K
Pressure:	0.001 bar
Raw Materials:	mol
Cl2(g)	2.0000E-01
TiC2	1.0000E+00
C	2.0000E+00

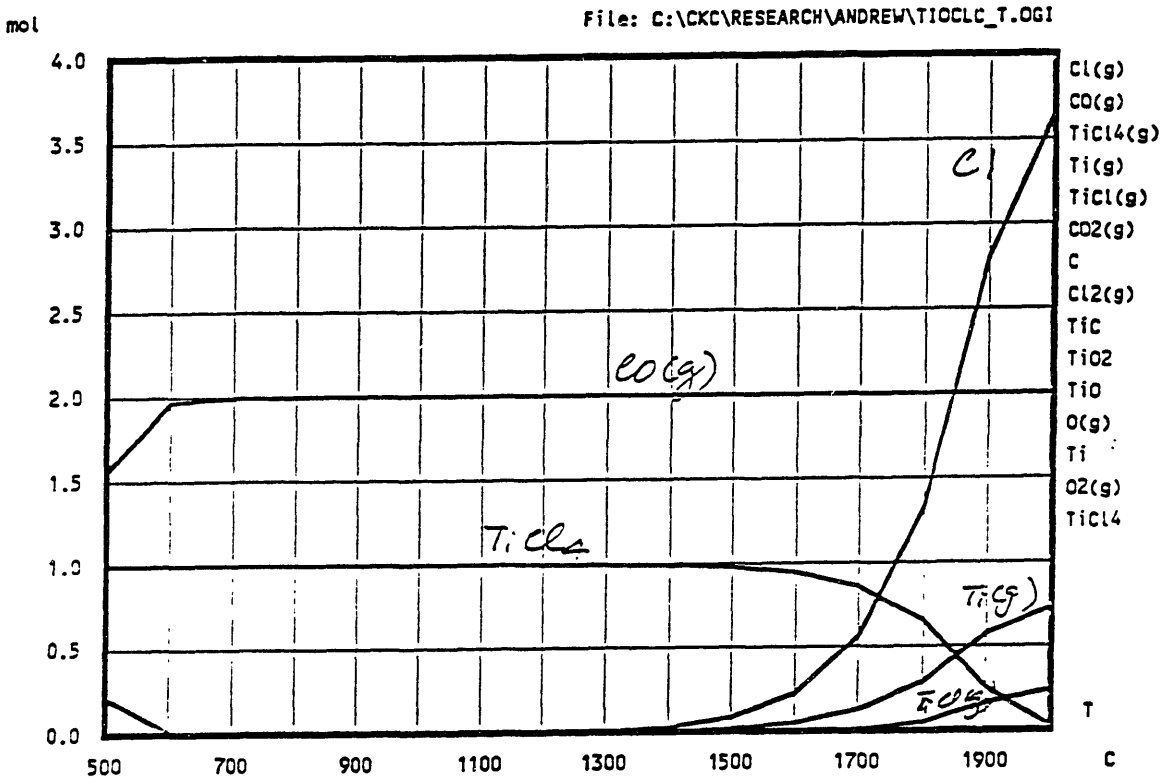

Temperature:	773.150 K
Pressure:	0.001 bar
Raw Materials:	mol
Cl2(g)	2.0000E+00
TiO2	1.0000E+00
C	2.0000E+00

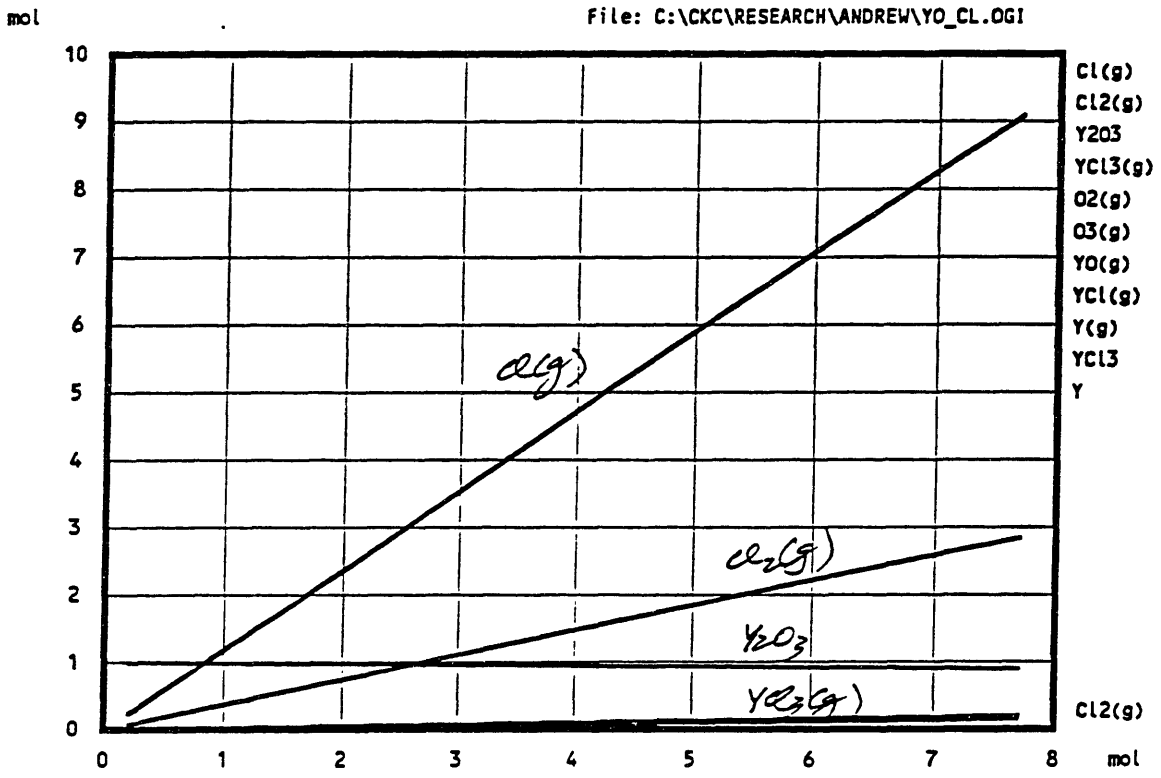

Temperature:	1473.150 K
Pressure:	0.001 bar
Raw Materials:	mol
Cl2(g)	2.0000E-01
Y2O3	1.0000E+00

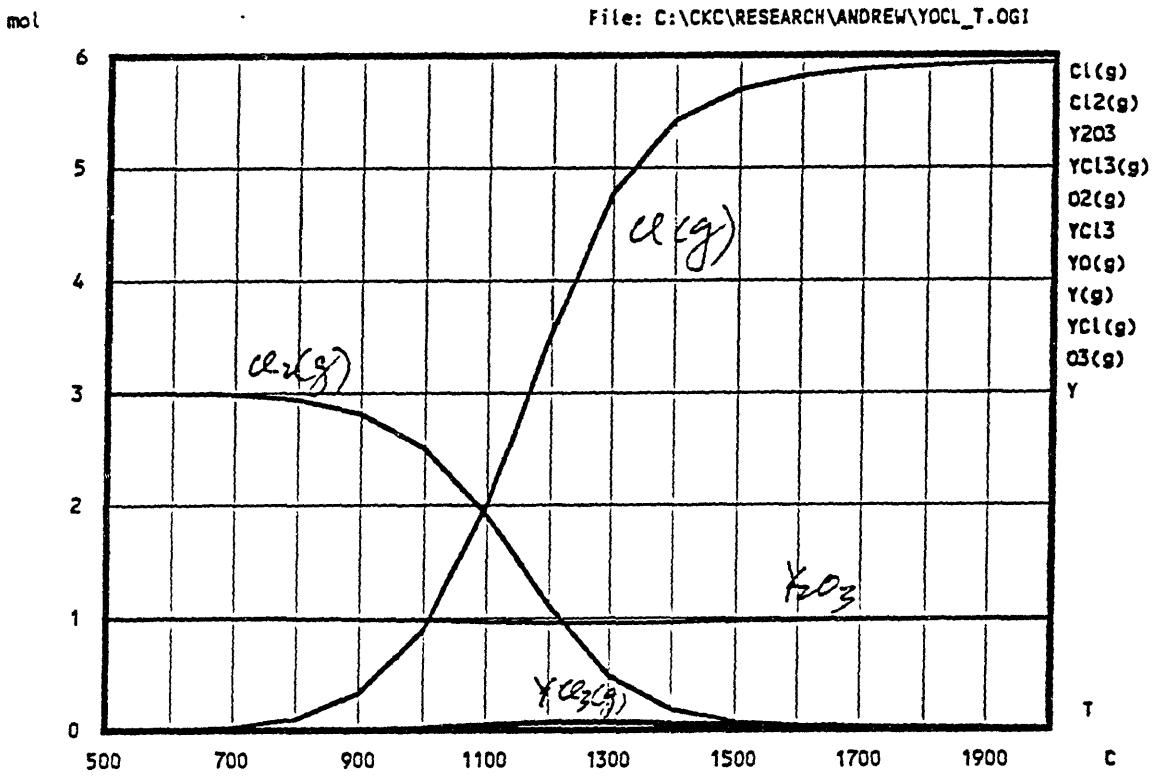

Temperature:	773.150 K
Pressure:	0.001 bar
Raw Materials:	mol
Cl2(g)	3.0000E+00
Y2O3	1.0000E+00

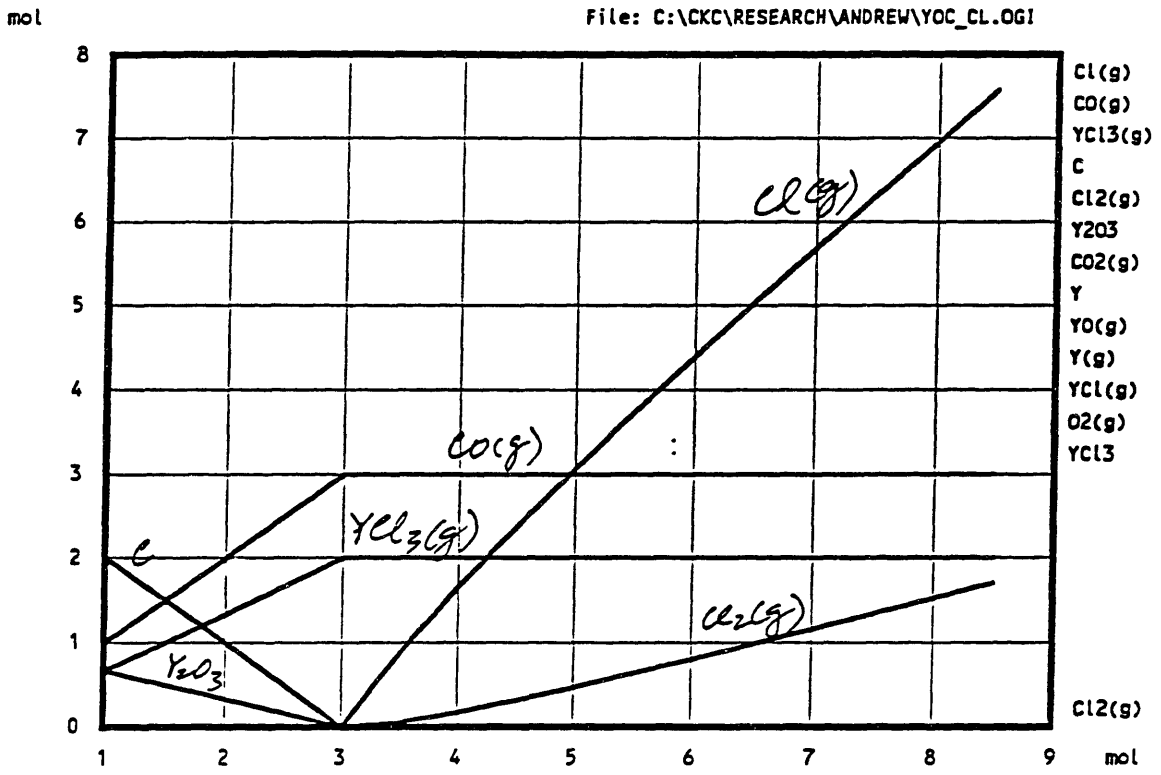

Temperature:	1473.150 K
Pressure:	0.001 bar
Raw Materials:	mol
Cl2(g)	1.0000E+00
Y2O3	1.0000E+00
C	3.0000E+00

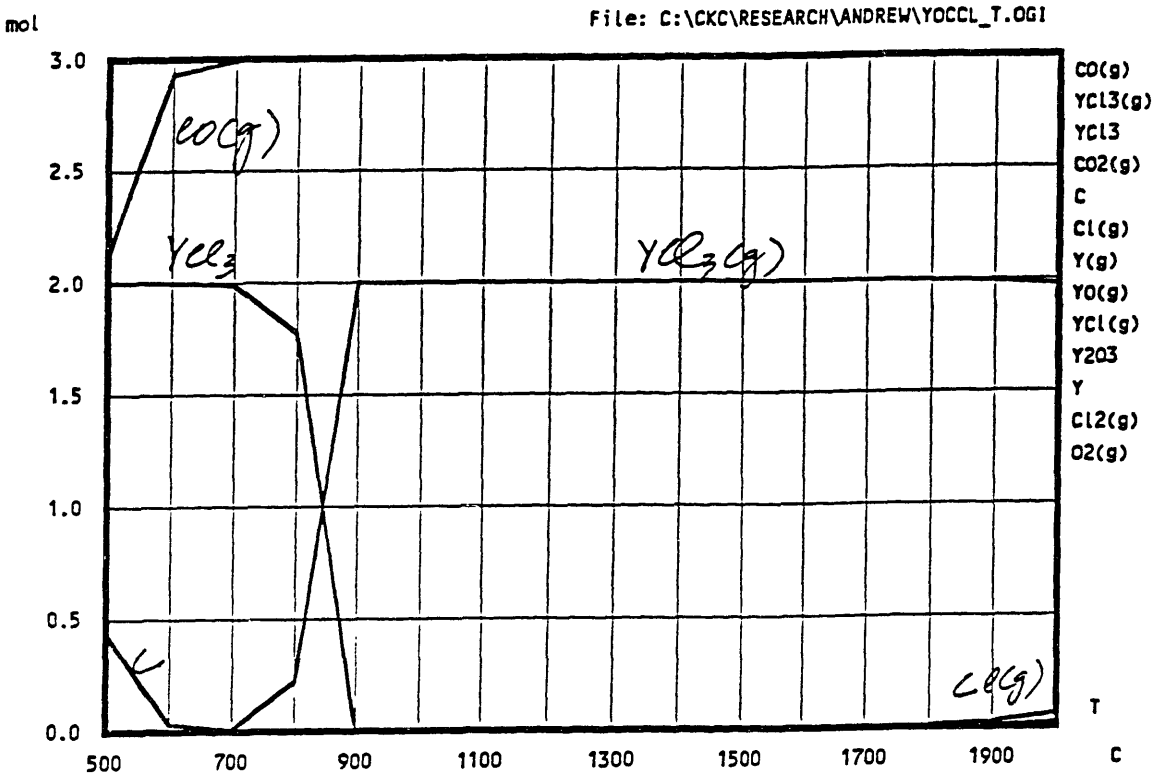

Temperature:	773.150 K
Pressure:	0.001 bar
Raw Materials:	mol
Cl2(g)	3.0000E+00
Y2O3	1.0000E+00
C	3.0000E+00

APPENDIX B. Results from Mercury Porosimetry

Table 3: Extracted Data from Porosimeter

	sample 1	sample 2	sample 3
Total intrusion volume (ml/g)	0.0331	0.0348	0.0358
Total pore area (m^2/g)	0.125	0.103	0.135
Median pore diameter (volume)(μm)	1.7534	2.2927	1.7513
Median pore diameter (area)(μm)	0.5775	0.6939	0.6373
Average pore diameter (4V/A)(μm)	1.0578	1.3545	1.0635
Bulk density(g/ml)	4.6589	4.8185	6.1693
Apparent skeletal density (g/ml)	5.5085	5.7896	7.9181
Porosity	15.42%	16.77%	22.09%